Geologica Acta, Vol.2, Nº3, 2004, 235-251
Available online at www.geologica-acta.com

geologica acta

RETRASO, a code for modeling reactive transport in saturated and unsaturated porous media

M.W. SAALTINK [1] F. BATLLE [1] C. AYORA [2] J. CARRERA [1] and S. OLIVELLA [1]

[1] Dept. of Geotechnical Engineering and Geosciences, School of Civil Engineering, Technical University of Catalonia (UPC)
C/ Jordi Girona 1-3, building D-2, 08034 Barcelona, Spain. Saaltink E-mail: maarten.saaltink@upc.es Batlle E-mail: francisco.batlle@upc.es Carrera E-mail: jesus.carrera@upc.es

[2] Institute of Earth Sciences Jaume Almera, Spanish Research Council (CSIC)
C/ Lluís Solé i Sabarís, s/n, 08028 Barcelona, Spain. E-mail: cayora@ija.csic.es

ABSTRACT

The code RETRASO (REactive TRAnsport of SOlutes) simulates reactive transport of dissolved and gaseous species in non-isothermal saturated or unsaturated problems. Possible chemical reactions include aqueous complexation (including redox reactions), sorption, precipitation-dissolution of minerals and gas dissolution. Various models for sorption of solutes on solids are available, from experimental relationships (linear K_D, Freundlich and Langmuir isotherms) to cation exchange and surface complexation models (constant capacitance, diffuse layer and triple layer models). Precipitation-dissolution and aqueous complexation can be modeled in equilibrium or according to kinetic laws. For the numerical solution of the reactive transport equations it uses the Direct Substitution Approach. The use of the code is demonstrated by three examples. The first example models various sorption processes in a smectite barrier. The second example models a complex chemical system in a two dimensional cross-section. The last example models pyrite weathering in an unsaturated medium. .

KEYWORDS | Reactive transport. Porous media. Unsaturated flow modeling. Numerical methods.

INTRODUCTION

The understanding of groundwater quality and the processes undergone by rocks in natural systems, the study of soil and groundwater contamination and the performance assessment of waste disposal facilities require quantitative analyses of the migration of reactive substances in soil and groundwater. This in turn requires the use of modeling tools which consider the concentrations of several chemical species and are able to model flow of groundwater and transport of solutes in groundwater by means of advection, dispersion and diffusion together with chemical reactions, such as acid-base reactions, redox reactions, complexation, biodegradation, adsorption, cation exchange and precipitation/dissolution of minerals. Moreover, in soils one has to consider unsaturated flow and transport processes in the gas phase, of which diffusion is of particular importance.

The last decades have witnessed considerable progress

on reactive transport modeling. Mangold and Tsang (1991) and, more recently, Van der Lee and De Windt (2001) have written reviews on this subject. Reactive transport involves many chemical species with complex interactions with each other through many chemical reactions. Rubin (1983) was the first in discussing mathematical formulations of the problem that make use of equilibrium constraints to reduce the problem complexity. Later, several authors presented algebraic manipulations of matrices and vectors (Friedly and Rubin, 1992; Steefel and MacQuarrie, 1996; Chilakapati et al., 1998). Finally, Saaltink et al. (1998) extended the use of such manipulations to reduce the number of variables to the minimum, that is, to the degrees of freedom, according to the phase rule.

The mathematical equations for reactive transport are highly non-linear. This, together with the large number of unknowns, may easily lead to excessive computation times, which makes it important to choose an appropriate approach to solve them. Several approaches are available. However, one can consider them to be variants of two families of methods. The first one is the operator splitting or two-step approach, which includes the Sequential Iteration Approach (SIA) and the Sequential Non Iteration Approach (SNIA). It consists of solving separately chemical equations and transport equations. The difference between SIA and SNIA is that the first approach iterates between these two types of equations to obtain a convergent solution, whereas the second does not. The second approach is the one-step, global implicit or Direct Substitution Approach (DSA). It consists of substituting the chemical equations into the transport equations and solving them simultaneously, usually by means of the Newton-Raphson method. In an article, which had a great impact, Yeh and Tripathi (1989) stated, "only those models that employ the SIA can be used for realistic applications". However, this has been criticized. Steefel and Lasaga (1994) wrote, "there are pros and cons to both methods, but the choice is less clearcut in favor of the decoupled methods than suggested by Yeh and Tripathi (1989)" and Van der Lee and De Windt (2001) called the statement "outdated". Moreover, Saaltink et al. (2001) showed that the SIA may require very small time steps to converge, where DSA can reach convergence in larger time steps due to its robustness. Nevertheless, the SIA may be faster when large grids of two or three dimensions are used. More importantly, the structure of SIA is easier to write in a modular form than that of DSA, which is advantageous from a programming point of view.

Many model codes have been developed. Most of them use the SIA. Examples are HYDROGEOCHEM (Yeh and Tripathi, 1991), MST1D (Engesgaard and Kipp, 1992), OS3D (Steefel and Yabusaki, 1995), TBS (Schäfer et al., 1998), FEREACT (Tebes-Stevens et al., 1998), TRANQUI (Xu et al., 1999) and HYTEC (Van der Lee et al., 2003). Examples of model codes that use the SNIA are DYNAMIX (Liu and Narasimhan, 1989a), MINTRAN (Walter et al., 1994), PHREEQM (Appelo and Willemsen, 1987), PHREEQC (Parkhurst, 1995), MOC-PHREEQE (Engesgaard and Traberg, 1996), and DIAPHORE (Le Gallo et al., 1998). Only few model codes use the DSA. Examples are TOUGH2 (White, 1995), GIMRT (Steefel and Yabusaki, 1995) and ARASE (Grindrod and Takase, 1996).

Modeling of reactive transport in the unsaturated zone has started more recently. Šimůnek and Suarez (1994) developed the code UNSATCHEM-2D for modeling major ion chemistry in variably saturated porous media; Wunderly et al. (1996) coupled the code PYROX, which describes oxygen diffusion and pyrite oxidation in an unsaturated zone, to MINTRAN. This coupled code was applied to study the effects of spatial heterogeneity on water quality (Gerke et al. 1998) and to model the drainage of a mine impoundment (Bain et al. 2000). These codes assume local equilibrium for all the chemical reactions. More recently, however, Mayer et al. (2002) developed the code MIN3P, which is able to model reactive transport in a saturated or unsaturated domain without assuming local equilibrium between minerals and water.

The objective of this paper is to present the coupling of a former reactive transport code RETRASO (Saaltink et al., 1997) with a multiphase flow and heat code CODE-BRIGHT (Olivella et al., 1996). This results in a new tool that can handle both saturated and unsaturated flow, heat transport and reactive transport in both liquid and gas. Although CODE-BRIGHT also permits the modeling of deformation or mechanical processes, this was not incorporated into the new code. Chemical reactions that can be modeled include aqueous complexation (including redox reactions), adsorption, precipitation-dissolution of minerals and gas dissolution. One, two and three-dimensional finite elements can be used for the spatial discretization. It uses the Direct Substitution Approach for the numerical solution of the reactive transport equations. This method also may fail to converge (although less than the Sequential Iteration Approach). Therefore, the time step is automatically reduced if convergence is not achieved. The last two features make RETRASO especially suitable for highly non-linear cases. A user-friendly interface is used in order to facilitate pre- and post-processing of the input and output data.

We start by explaining the mathematical equations that describe the (un)saturated flow processes, the chemical reactions and the reactive transport processes. Then, we explain the verification of the code, followed by examples of applications of RETRASO. The last section contains our conclusions.

FLOW AND HEAT TRANSPORT EQUATIONS

The flow problem is formulated in a multiphase approach, that is, a porous media composed of solid grains, water and gas. Within this porous media, thermal and hydraulic aspects will be taken into account, interacting simultaneously and considered in an integrated way. Three phases are considered: solid phase (mineral), liquid phase (water and dissolved air), gas phase (mixture of dry air and water vapor). Three components are considered: water, dry air and heat. Mass balance equations are formulated for each component. To each mass balance a state variable is associated: liquid pressure (P_l in Pa), gas pressure (P_g in Pa) and temperature (T in K). Constitutive laws have to be used to express the mass balance equations as function of the state variables.

Balance equations

The total mass balance of water is expressed as:

$$\frac{\partial}{\partial t}\left(\omega_l^w \rho_l S_l \phi + \omega_g^w \rho_g S_g \phi\right) + \nabla \cdot \left(\mathbf{j}_l^w + \mathbf{j}_g^w\right) = f^w \qquad (1)$$

where subscripts l and g refer to liquid and gas and superscript w to water, ω is the mass fraction (kg kg^{-1}) of a component in a phase, ρ is the density (kg m^{-3}) of a phase, S is the hydraulic saturation (m^3 m^{-3}), ϕ is the porosity (m^3 m^{-3}), $\mathbf{j}$ (kg m^{-2} s^{-1}) is the total flux (advective, dispersive and diffusive) and f is an external source/sink term (kg m^{-3} s^{-1}). Note that the first term represents the change of mass of water in the liquid phase, the second term represents the change of mass of water in the gas phase (i.e., vapor) and the third and fourth terms represent the transport of water in liquid and the gas phase, respectively.

Similar to the mass balance of water, the mass balance of air can be expressed as:

$$\frac{\partial}{\partial t}\left(\omega_l^a \rho_l S_l \phi + \omega_g^a \rho_g S_g \phi\right) + \nabla \cdot \left(\mathbf{j}_l^a + \mathbf{j}_g^a\right) = f^a \qquad (2)$$

where superscript a refers to air.

The equation for internal energy balance for the porous medium is established taking into account the internal energy in each phase (E_s, E_l, E_g in J kg^{-1}):

$$\frac{\partial}{\partial t}\left(E_s \rho_s (1-\phi) + E_l \rho_l S_l \phi + E_g \rho_g S_g \phi\right) + \nabla \cdot (\mathbf{i}_c + \mathbf{j}_{Es} + \mathbf{j}_{El} + \mathbf{j}_{Eg}) = f^Q \qquad (3)$$

where $\mathbf{i}_c$ is energy flux (J m^{-2} s^{-1}) due to conduction through the porous medium, the other fluxes ($\mathbf{j}_{Es}$, $\mathbf{j}_{El}$, $\mathbf{j}_{Eg}$) are advective fluxes (J m^{-2} s^{-1}) of energy caused by mass motions and f^Q is an internal/external energy supply (J m^{-3} s^{-1}).

Constitutive equations and equilibrium restrictions

A set of constitutive and equilibrium laws are required to express the various parameters or dependent variables of the mass balance equation (ω, ρ, S, E, $\mathbf{j}$, $\mathbf{i}_c$, etc.) as function of the state variables or independent variables (P_l, P_g and T). Table 1 gives a summary of constitutive laws and equilibrium restrictions that should be incorporated in the general formulation. It also shows the dependent variables that are computed using each of the laws. Below we explain some of the most important constitutive and equilibrium laws.

Generalized Darcy's law has been used to compute the advective flux of the α phase (α=l for liquid, α=g for gas):

$$\mathbf{q}_\alpha = -\frac{\mathbf{k} k_{r\alpha}}{\mu_\alpha}\left(\nabla P_\alpha - \rho_\alpha \mathbf{g}\right) \qquad (4)$$

where $\mathbf{k}$ is the tensor of intrinsic permeability (m^2), k_{ra} is the relative permeability of the phase, μ_a is the phase's dynamic viscosity (Pa s) and $\mathbf{g}$ is the gravity vector (m s^{-2}).

Fick's law has been used to compute the diffusive flux of component β in phase α:

$$\mathbf{i}_\alpha = -\phi \tau \rho_\alpha S_\alpha D_\alpha^\beta \mathbf{I} \nabla \omega_\alpha^\beta \qquad (5)$$

where τ is a tortuosity parameter, D_a is the molecular diffusion coefficient (m^2 s^{-1}) which is a function of

TABLE 1 | **Constitutive equations and equilibrium restrictions.**

Equation	Variable Name	Variable
Constitutive equation		
Darcy's law	liquid and gas advective flux	$\mathbf{q_l}$, $\mathbf{q_g}$
Fick's law	vapour and air non-advective fluxes	$\mathbf{i_g^w}$, $\mathbf{i_l^a}$
Fourier's law	conductive heat flux	$\mathbf{i_c}$
Retention curve	Liquid phase degree of saturation	S_l, S_g
Phase density	liquid density	ρ_l
Gases law	gas density	ρ_g
Equilibrium restrictions		
Henry's law	Air dissolved mass fraction	ω_l^a
Psychrometric law	Vapour mass fraction	ω_g^w

temperature and phase pressure and **I** is the identity matrix.

Various sets of retentions curves expressing saturation as a function of liquid or gas pressure can be used, such as the Van Genuchten's (Van Genuchten, 1978):

$$S_l = \left(1 + \left(\frac{P_g - P_l}{P_0}\right)^{\frac{1}{1-n}}\right)^{-n} \qquad (6)$$

$$S_g = 1\text{-}S_1$$

where P_0 and n are scale pressure and shape parameters, respectively.

The relative permeability (k_{ra}) in eq. 4 is a function of the saturation. As for the retention curve, various expressions exist, but that of Van Genuchten is the most widely used.

$$k_{rl} = \sqrt{S_l}\left(1 - \left(1 - S_l^{1/n}\right)^n\right)^2 \qquad (7)$$

where n has the same meaning as for eq. 6, although it does not necessarily has the same value.

Constitutive laws may contain physical parameters that, in their turn, are functions of state variables. For instance, in eq. 4 the dynamic viscosity (μ_a) highly depends on temperature and the relative permeability (k_{ra}) depends on saturation (S_l) through eq. 7, which in its turn depends on pressures (P_l and P_g) through eq. 6.

CHEMICAL EQUATIONS

Equilibrium approach

Species, reactions and stoichiometric coefficients

A chemical system is made up of a set of atomic constituents or elements. A chemical species is defined as any chemical entity distinguishable from the rest due to its elemental composition, and the phase at which it is present. For instance, CO_2 gas is a different species than dissolved CO_2.

Not all species are needed to fully describe the chemical system. The subset of species which is strictly necessary is made up of what are known as components. These components can be chosen arbitrarily among all species. Although the N_e atomic constituents could serve as a set of components, they are never used as such because the constituents themselves are rarely present in aqueous phases. For this reason, it is more convenient to select as components a subset of N_c chemical species. These species are also known as the primary species.

In a system made up of N_s chemical species, any of the N_r reactions taking place can be represented as a linear combination such as

$$\sum_{j=1}^{N_s} \nu_{ij} Q_j \qquad i = 1, \ldots, N_r \qquad (8)$$

where Q_j is the chemical formula of the j-th species, and n_{ij} is its stoichiometric coefficient in reaction i. The matrix **S** of stoichiometric coefficients is a $N_r \times N_s$ rectangular matrix having a range equal to N_r. **S** has the form:

$$\mathbf{S} = \begin{pmatrix} \nu_{11} & \nu_{12} & \cdots & \nu_{1N_c} & -1 & 0 & \cdots & 0 \\ \nu_{21} & \nu_{22} & \cdots & \nu_{2N_c} & 0 & -1 & \cdots & 0 \\ \vdots & \vdots & \ddots & \vdots & \vdots & \vdots & \ddots & \vdots \\ \nu_{N_r 1} & \nu_{N_r 2} & \cdots & \nu_{N_r N_c} & 0 & 0 & \cdots & -1 \end{pmatrix} \qquad (9)$$

where the **–I** matrix stands for the decomposition reaction of the secondary (non-primary) species (in the aqueous solid or gas phase). In RETRASO the entries v_{ij} of the submatrix **S*** (**S = S* -I**) are obtained from a thermodynamic database by defining a set of aqueous species as a primary species. The code checks that this set of species is independent and able to form the rest of species, called secondary species (aqueous complexes, minerals, gases, surface complexes), a linear combination of primary species.

Aqueous complexation reactions

The continuous motion of dissolved ions together with their large number per unit volume cause numerous collisions making possible the formation of ion pairs and/or dissolved complexes which usually have an ephemeral live (on the order of 10^{-10} s). Since these reactions are almost instantaneous, they can be effectively considered as equilibrium reactions. The equilibrium constant relates the average number of ions pairs or complexes which are being formed. Applying the mass action law yields:

$$\log \mathbf{K_a} = \mathbf{S_a} \log \mathbf{c_a} + \mathbf{S_a} \log \gamma_a(\mathbf{c_a}) \qquad (10)$$

where $\mathbf{K_a}$ is the equilibrium constant vector, which only

depends on temperature and pressure, $\mathbf{S}_a$ is the stoichiometric coefficient matrix for aqueous complexation reactions, $\mathbf{c_a}$ is the molal concentration vector of aqueous species and γ_a is the vector of thermodynamic activity coefficients, calculated from $\mathbf{c_a}$ according to the B-dot expression (Helgeson and Kirkham, 1974).

Equation 10 allows the calculation of the concentration of secondary aqueous species, $\mathbf{c_{a2}}$, from the set of concentrations of N_c primary species $\mathbf{c_{a1}}$:

$$\log \mathbf{c}_{a2} = \log \mathbf{K}_a + \mathbf{S}_a^* \log \mathbf{c}_{a1} + \mathbf{S}_a^* \log \gamma_a(\mathbf{c}_a) \quad (11)$$

The transfer of electrons between two different atoms changes their chemical valence. This transfer is known as an oxidation-reduction reaction. RETRASO describes redox reactions by assuming the electron as an aqueous component or a master species. Contrary to the protons, which exist in reality as dissolved species, the electron concentration is a hypothetical variable. This allows to complete the redox half-reactions and treat them as the rest of the chemical reactions in the aqueous phase. Each half redox reaction is completed by adding electrons as transferable species. The activity coefficient of this hypothetical species is assumed to be equal to one.

Sorption reactions

In a first step, sorption of solutes on solid phases has been described as experimental relationships such as lineal K_D, Freundlich and Langmuir equations. More elaborated mechanistic models to describe sorption are surface complexation and ion exchange models. Although RETRASO may calculate experimental equations, we only describe here the mechanistic models.

The sorption of solute at the solid surfaces is described as chemical reactions between the aqueous species and specific surface sites (surface complexation). These surface reactions include proton exchange, cation binding and anion binding via ligand exchange at surface hydroxide sites (represented here as XOH). For example, the desorption of a metal could be represented as:

$$XOM^{z-1} + H^+ = XOH + M^z$$

These reactions are fast with respect to flow and are commonly assumed in equilibrium. Therefore, they can be treated according to the mass action law (10). However, in aqueous complexation reactions the electric charge is homogeneously distributed in the solution, whereas surface reactions take place on a fixed charged surface, which creates an electrostatic field. An additional energetic term accounting for the work needed for the aqueous species to travel across the surface electric field is required:

$$\Delta G^0_{ads} = \Delta G^0_{\text{int}} + \Delta z F \psi_0 \quad (12)$$

where, ΔG^0_{ads} is the standard free enthalpy change of the overall adsorption reaction, ΔG^0_{intr} is the standard free enthalpy change due to chemical bonding and the last term is the electrostatic work. Δz is the change in the charge of the surface species, F the Faraday's constant (96485 C/mol) and ψ_0 is the mean surface potential (V). Eq. (12) can be rewritten as:

$$K_{ads} = K_{\text{int}} e^{-\frac{\Delta z F \psi_0}{RT}} \quad (13)$$

where, R is the gas constant (8.314 J/mol/K) and T the absolute temperature (K), K_{ads} the equilibrium constant of the overall adsorption process and K_{intr} does not depend on the surface charge.

By considering the electrostatic term in the equilibrium formulation a new unknown, the mean surface potential (ψ_0), is introduced. This value depends on the total charge accumulated on the surface. Several theoretical models describe the dependence of ψ_0 on the charge density. With increasing order of complexity, the models included in RETRASO are: the constant capacitance, the diffuse layer and the triple layer model (Westall and Hohl, 1980; Dzombak and Morel, 1990) . The option for a particular model depends on the amount of experimental data needed to obtain the equilibrium constant of the reactions.

The concentration of a sorbed species (c_d) (mol/kg water) can be expressed in terms of the concentration of

$$\log \mathbf{c}_d = -\log \mathbf{K}_d + \begin{pmatrix} \mathbf{S}_d^* & \mathbf{S}_x^* \end{pmatrix} \begin{pmatrix} \log \mathbf{c}_{a1} \\ \log \mathbf{c}_x \end{pmatrix} + \mathbf{S}_d^* \log \gamma_{a1} \quad (14)$$

where K_d is the equilibrium constant of the desorption reaction, $\mathbf{S_d}^*$ is the submatrix of stoichiometric coefficients of the desorption reactions ($N_d \times N_c$). In order to represent the adsorbed species an additional set of N_x components has to be added to the initial set of N_c aqueous primary species. N_x can be 4 (triple layer model), 2 (double layer and constant capacitance models), or 1 (non electrostatic). Then, $\mathbf{S_x}^*$ is a submatrix ($N_d \times N_x$), whose first column contains the stoichiometric coefficients of the empty surface sites (XOH) of the desorption reactions, and the rest of columns the Δz of the electrostatic term of eq. 13. Vector $\mathbf{c_x}$ contains the values of the additional primary species: $c_x(1)$, the concentration of the empty surface sites, and $c_{\mathbf{x}}(2)$ to $c_{\mathbf{x}}(4)$, terms of the shape ($-F\psi_0/RT$).

Cation exchange takes place when an exchangeable cation located in structural positions of minerals is

exchanged with a cation in the solution. The main difference with the surface complexation model is the fact that no free sorption sites are assumed, and the capture of a cation from the solution is always coupled with the release of a cation from the surface.

The concentration of sorbed species can be calculated according to the eq. 14, with no electrostatic terms. The activity of the sorbed species are not assumed equal to concentration, but calculated according to several conventions: Gaines-Thomas, Gapon or Vanselow (Appelo and Postma, 1994). According to the Gaines-Thomas convention the activity of an exchangeable cation is equated with its equivalent fraction:

$$a_d = \frac{z_d c_d}{CEC} \quad (15)$$

where c_d is the concentration of sorbed species (mol/kg water), z_d is electric charge of the cation and *CEC* is the cation exchange capacity (in eq/ kg water).

Solid-liquid interactions

Under equilibrium conditions, dissolution-precipitation reactions can be described by the law of mass action which states that

$$\log \mathbf{X_m} + \log \gamma_\mathbf{m} + \log \mathbf{K_m} = \mathbf{S_m^*} \log \mathbf{c_{a1}} + \mathbf{S_m^*} \log \gamma_{\mathbf{a1}} \quad (16)$$

where $\mathbf{X_m}$ is the vector of molar fraction of the *m*-th species a solid phase, $\gamma_\mathbf{m}$ is its thermodynamic activity coefficient ($\mathbf{X_m}$ and $\gamma_\mathbf{m}$ are taken equal to 1 for pure phases), and $\mathbf{S_m}^*$ is the submatrix of stoichiometric coefficients of the dissolution reactions ($N_m \times N_{a1}$, N_m being the number of minerals), and $\mathbf{K_m}$ is the vector of equilibrium constants.

The equilibrium condition only provides a relationship among the concentrations of the involved aqueous species. The mass transfer, $\mathbf{c}_\mathrm{m}$, (mass of solid species dissolved or precipitated) is not specified. Therefore, RETRASO does not solve the mineral equilibrium equations for $\mathbf{X_m}$ but uses eq. (16) to reduce the number of transport equations (see section on reactive transport equations).

Gas-liquid interactions

We assume that all gas-liquid reactions are sufficiently fast with respect to flow to reach equilibrium. Then, the mass action law states that

$$\log \mathbf{p_f} = -\log \mathbf{K_f} - \log \gamma_\mathbf{f} + \mathbf{S_f^*} \log \mathbf{c_{a1}} + \mathbf{S_f^*} \log \gamma_{\mathbf{a1}} \quad (17)$$

where $\mathbf{p_f}$ is the vector of partial pressure of the gas species in the gas phase, $\gamma_\mathbf{f}$ are their activity coefficients, $\mathbf{S_f^*}$ is the submatrix of stoichiometric coefficients of the gas dissolution reactions ($N_f \times N_{a1}$), and $\mathbf{K_f}$ is the vector of equilibrium constants.

For low pressures (in the range of atmospheric pressure), the gaseous phase behaves like an ideal mixture ($\gamma_\mathbf{f} = 1$). Then, the chemical equilibrium between a species in the aqueous phase and in the gas phase can be represented by Henry's law:

$$p_f = \frac{\gamma_a}{K_f} c_a \quad (18)$$

where the fraction is the so called Henry's constant, which has units of (bar kg_{water}/mol) and depends on the ionic strength of the solution. Moreover, the partial pressure p_f is equal to the total pressure times the molar fraction X_f (Dalton's law). The sum of the partial pressures (p_f) of all gaseous species equals the pressure of the gas phase (P_g):

$$P_g = \sum_f p_f \quad (19)$$

At low pressures, not only the mixture behaves as ideal, but also each species respects the ideal gas equation:

$$p_f V = n_f RT \quad (20)$$

so that we can write the concentration of the chemical species in the gas phase (c_f), expressed in moles per unit of volume, as:

$$c_f = \frac{p_f}{RT} \quad (21)$$

Kinetic approach

Some geochemical processes are known to progress so slowly with respect to fluid flow that they may never reach equilibrium, such as dissolution and precipitation of many minerals. Also aqueous complexation reactions, particularly redox reactions, cannot always be assumed to be in equilibrium. For instance, equilibrium between aqueous redox species such as Fe^{2+} and Fe^{3+}, which is commonly assumed in conventional geochemical calculations, may be not true in nature (Nordstrom and Alpers, 1999) and hence, should not be assumed. A realistic estimate of Fe^{3+} concentration would be also of interest, as Fe^{3+} along with O_2 can oxidize pyrite as well as precipitate in secondary minerals.

Contrary to the equilibrium approach, the kinetic expression does provide an explicit way to compute the amount of reactants and products per unit of volume and unit of time. This is expressed through a kinetic rate law. For kinetic reactions involving minerals, RETRASO uses a general formulation, which includes several types of experimental functions (Steefel and Lasaga, 1994):

$$r_k = \sigma_k \zeta_k e^{-\frac{E_{a,k}}{RT}} \sum_{j=1}^{N_k} k_{kj} \prod_{i=1}^{N_c+N_s} a_i^{p_{kji}} \left(\Omega_k^{\theta_{kj}} - 1\right)^{n_{kj}} \quad (22)$$

where r_k is the mineral dissolution rate (moles of mineral per unit of volume and unit time), $E_{a,k}$ is the apparent activation energy of the overall reaction process; N_k is the number of terms of the experimental expression, and k_{kj} an experimental constant; $a_i^{p_{kji}}$ accounts for the catalytic effect of some species (particularly of H^+), where the value of p_i is determined experimentally; Ω_k is saturation index for the k-th mineral reaction; the parameters θ and η must be determined from experiments; usually but not always they are taken equal to 1. The term inside the parenthesis, called the far-from-equilibrium function, decreases the reaction rate in a non-linear way, as the solution approaches to equilibrium. Factor ζ_k takes on values of +1 or -1 depending on whether Ω_k is larger or smaller than 1 (precipitation or dissolution), respectively. At equilibrium, $\Omega_k = 1$ and therefore $r_k = 0$. σ_k is the reactive surface of the mineral per unit of volume. RETRASO permits the change of σ_k in time due to changes of the mineral concentrations.

For kinetic aqueous complexation reactions no reactive surface and no far-from-equilibrium function should be incorporated. This can be achieved by simply setting σ_k to 1 and η to 0.

REACTIVE TRANSPORT EQUATIONS

We used the mathematical formulation for reactive transport of Saaltink et al. (1998), to which we added terms for the transport and chemistry of gaseous species. Then, the reactive transport equations can be written as:

$$\mathbf{U_a} \frac{\partial \phi S_l \rho_l \mathbf{c_a}}{\partial t} + \mathbf{U_d} \frac{\partial \phi \rho_l \mathbf{c_d}}{\partial t} + \mathbf{U_m} \frac{\partial (1-\phi)\rho_s \mathbf{c_m}}{\partial t} + \mathbf{U_g} \frac{\partial \frac{\phi S_g}{RT} \mathbf{p_f}}{\partial t} =$$

$$= \mathbf{U_a} L_l(\mathbf{c_a}) + \mathbf{U_f} L_g(\mathbf{p_f}) + \mathbf{U S_k^t r_m}(\mathbf{c_a}) \quad (23)$$

Equations 23 are the N_c overall reactive transport equations. Vectors $\mathbf{c_a}$, $\mathbf{c_d}$, $\mathbf{c_m}$ (mol kg^{-1}) and $\mathbf{p_f}$ (Pa) are the concentrations of aqueous species, adsorbed species, minerals and partial pressures of gaseous species, respectively. Matrix $\mathbf{S_k}$ and vector $\mathbf{r_k}$ contains the stoichiometric coefficients and the rates of the kinetic reactions, which can be considered as functions of all aqueous concentrations. Matrices $\mathbf{U_a}$, $\mathbf{U_d}$, $\mathbf{U_m}$ and $\mathbf{U_g}$ are called the component matrices for aqueous, sorbed, mineral and gaseous species and relate the concentrations of the species with the total concentrations of the components. The matrix $\mathbf{U}$ is the component matrix for all species. These matrices can be computed from the stoichiometric coefficient of the chemical reactions. An exception are columns of these matrices that refer to the electron (e^-) involved in redox reactions. The use of e^- stems from writing a redox reaction as two half-reactions. This is useful for mass action laws, but in reality there is no free electron in the solution (its real concentration equals zero). Therefore, the columns of the component matrix that refer to the electron must be set to zero.

By using mineral equilibrium equations we can eliminate N_m of the N_c transport equations as explained in more detail by Saaltink et al. (1998). This is achieved by multiplying equations by matrix $\mathbf{E}$, kernel of $\mathbf{U_m}$ (i.e., $\mathbf{EU_m = 0}$). This eliminates the concentrations of minerals in equilibrium and reduces the number of transport equations per node to N_c - N_m. The resulting transport equations are denoted:

$$\mathbf{EU_a} \frac{\partial \phi S_l \rho_l \mathbf{c_a}}{\partial t} + \mathbf{EU_d} \frac{\partial (1-\phi)\rho_s \mathbf{c_d}}{\partial t} + \mathbf{EU_g} \frac{\partial \frac{\phi S_g}{P_g} \mathbf{p_f}}{\partial t} =$$

$$= \mathbf{EU_a} L_l(\mathbf{c_a}) + \mathbf{EU_g} L_g(\mathbf{p_f}) + \mathbf{E U S_k^t r_k}(\mathbf{c_a}) \quad (24)$$

As explained in the previous section the variables $\mathbf{c_a}$, $\mathbf{c_d}$ and $\mathbf{p_f}$ can be written as function of N_c - N_m primary variables $\mathbf{c_i}$.

L_l and L_g are linear operators for the advection, dispersion/diffusion and non-chemical sink-source terms for the liquid and gas phase, respectively:

$$L_l() = -\nabla \cdot (\mathbf{q_l} \rho_l()) + \nabla \cdot (\mathbf{D_l} \phi S_l \rho_l \nabla()) + m_l \quad (25)$$

$$L_g() = -\nabla \cdot \left(\mathbf{q_g} \frac{1}{RT}()\right) + \nabla \cdot \left(\mathbf{D_g} \phi S_g \frac{P_g}{RT} \nabla \frac{()}{P_g}\right) + m_g \quad (26)$$

where m_l and m_g are the non-chemical sources-sinks (mol m^{-3} s^{-1}) and $\mathbf{D_l}$ and $\mathbf{D_g}$ are the dispersion/diffusion tensors (m^2 s^{-1}). In two dimensions these tensors are:

$$\mathbf{D}_{\alpha} = \begin{pmatrix} \frac{\alpha_{L,\alpha} v_{x,\alpha}^2 + \alpha_T v_{y,\alpha}^2}{|\mathbf{v}_{\alpha}|} & \frac{(\alpha_{L,\alpha} - \alpha_{T,\alpha}) v_{x,\alpha} v_{y,\alpha}}{|\mathbf{v}_{\alpha}|} \\ \frac{(\alpha_{L,\alpha} - \alpha_{T,\alpha}) v_{x,\alpha} v_{y,\alpha}}{|\mathbf{v}_{\alpha}|} & \frac{\alpha_{L,\alpha} v_{y,\alpha}^2 + \alpha_{T,\alpha} v_{x,\alpha}^2}{|\mathbf{v}_{\alpha}|} \end{pmatrix} + \mathbf{I} D_{0,\alpha} \tau_{\alpha} \quad (27)$$

where subscript α refers to the phase (l or g). For one dimension equation 27 reduces to:

$$\mathbf{D}_{\alpha} = \alpha_{L,\alpha} v_{x,\alpha} + D_{0,\alpha} \tau_{\alpha} \quad (28)$$

where α_L and α_T are the longitudinal and transversal dispersivities (m), $v_{x,a}$ and $v_{y,a}$ are the velocities (m s^{-1}) in x and y direction for phase α, D_0 is the molecular diffusion (m^2 s^{-1}) in the pure phase and τ is the tortuosity. RETRASO permits two functions to calculate the tortuosity, τ:

$$\tau = \sqrt{\phi S} \quad (29)$$

$$\tau = \frac{(\phi S)^{\frac{7}{3}}}{\phi^2} \quad (30)$$

The first term of the right-hand-sides of (27) and (28) represents dispersion and the second molecular diffusion. It is worth noting that, generally, in the liquid phase the dispersive term dominates, whereas in the gas phase the diffusive term dominates. The most correct would be to calculate the diffusion in the gas phase according to complex relations taking into account pressure, temperature, type of gaseous species and chemical composition of the gas as explained by Thorstenson and Pollock (1989), Baehr and Baker (1995) and Abu-El-Sha'r and Abriola (1997). We opted for calculating the gaseous diffusion coefficient, D_0, by assuming binary diffusion between every gaseous species and a majority species (usually N_2). Then the diffusion coefficient for gaseous species ($D_{0,g}$) becomes:

$$D_{0,g} = \frac{1.43 \cdot 10^{-2} T^{1.75}}{P_g \sqrt{2\left(w_i^{-1} + w_m^{-1}\right)^{-1}} \left(a_i^{\frac{1}{3}} + a_m^{\frac{1}{3}}\right)^2} \quad (31)$$

where w is the molecular weight in g/mole, a is the diffusion volume. Subscripts i and m refer to the considered gaseous species and the majority species. Diffusion coefficient, $D_{0,g}$, gas pressure, P_g, and temperature, T, are in m^2/s, Pa and K, respectively.

VERIFICATION

The conservative solute and heat transport subroutines of RETRASO have been verified for one dimensional condition. This 1-D test case corresponds to the time evolution of concentrations in a semi-infinite confined aquifer under steady-state uniform velocity flow regime. Under these conditions, the analytical solution is given by van Genuchten and Alves (1982).

Reactive transport with dissolution-precipitation reactions has been verified for 1D problems in saturated media. Gypsum and calcite dissolution under local equilibrium assumption gave solute concentrations very close to those given by a simple transport code coupled with PHREEQE with a two step approach. Reactive transport with kinetic rate laws was checked for calcite and smectite dissolution against the independent fully coupled code 1DREACT (Steefel, 1993).

For the purpose of verifying the capabilities of RETRASO to deal with redox processes, a case of uranium migration through a column was selected. This case was used to verify RETRASO against DYNAMIX (Liu and Narashimhan, 1989b).

Reactive transport with cation exchange routines was verified against a PHREEQM user's manual problem (Nienhuis et. al., 1991). The column, initially filled with 1 mM $NaNO_3$ and 0.2 mM KNO_3, is flushed by a 0.6 mM $CaCl_2$ solution. This case illustrates the chromatographic separation of Ca and K. Ca is weakly adsorbed and is eluted first. K is more tenaciously held than Ca and appears retarded in the column effluent.

To verify surface sorption modeling, an example of cadmium transport reported by Cederberg et al. (1985) was used. The transport of cadmium, chloride and bromide in a one-dimensional laboratory column was simulated. The physical and chemical processes considered included dispersion, advection, formation of complexes in the aqueous phase, and sorption of free cadmium. Sorption routines were also verified for Ni sorption in montmorillonite (see first demonstration case below).

DEMONSTRATION EXAMPLES

RETRASO has been applied to many reactive transport problems. It has been used, among others, to model diagenetic processes of rocks, such as dedolomitization (Ayora et al., 1998), and the formation of ore deposits (Corbella, 2002; Salas, 2002), for the analysis and parametrization of a deep well recharge experiment (Saaltink et al., 2003), for the interpretation of pyrite oxidation experiments (Saaltink et al., 2002), to simulate the retention of uranium in

column experiments (Rovira et al., 2000), and to understand the quality of groundwater samples around a uraninite deposit (Salas, 2002). It would take too much to describe them all. Instead, we selected three representative examples. The first example, on a smectite barrier, shows the capability of RETRASO to handle the various sorption models. The second example, Okélobondo, shows the potential of RETRASO to model a complex chemical system in a two dimensional cross-section. The last example, on pyrite weathering, demonstrates the capability of the code to handle reactive transport in combination with unsaturated flow.

Smectite barrier

A simple case of Ni diffusion through 1 m-thick bentonite barrier is calculated. The barrier is made up of 1/3 of Na-montmorillonite. A porosity of 0.4 and a Ni boundary concentration of 10^{-4} M Ni are assumed (Fig. 1). The sorption model is based on Baeyens and Bradbury (1997), and consists of four different sorption sites (cation exchange sites, one surface complexation site with strong affinity, and two with weak affinities).

Prior to reactive transport calculations, the correct functioning of the code was checked by comparing the calculated and the experimental values (Bradbury and Baeyens, 1997) of the evolution of the sorbed Ni with pH (Fig. 2). This was done by introducing several boundary waters with different pH. The contribution of the different sites to sorption is represented in Fig. 3. The model underpredicts the experimental sorbed values at high pH because the possible precipitation of $Ni(OH)_2$ is not included in the calculations.

The numerical model was 1D, with 100 nodes, a variable time increment, and a total time span of 10^4 years. Reactive transport calculations were performed for a conservative solute and for Ni. The exchange capacity was 0.96 eq/L, and the concentration of sorption sites in the bentonite were 2.20 mmol/L (strong), and 44.0 mmol/L (weak). The second weak sites did not sorb Ni. As shown in Fig. 4, the bentonite barrier was able to retain Ni during 10^4 years. After this period practically all Ni generated in

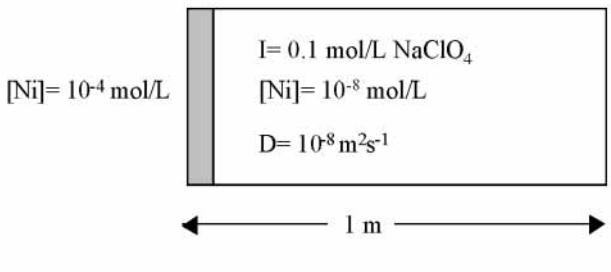

FIGURE 1| **Sketch of the modeling case of Ni diffusion through a bentonite barrier.**

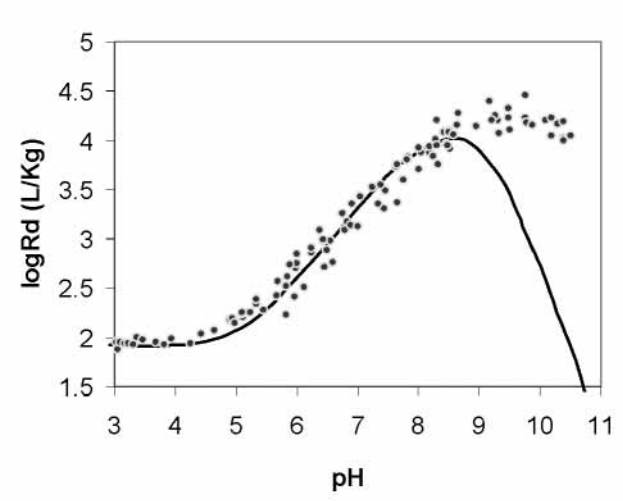

FIGURE 2| **Ni sorption versus pH in Na montmorillonite for I=0.1. The points are the experimental values (Bradbury and Baeyens, 1997) and the line the calculated values.**

the source reaches the external edge of the barrier. Since this model uses a fixed pH, the reactive transport can also be calculated with a related constant retardation factor. These calculations can be used for code verification. Both calculations gave practically identical results (Fig. 4).

Okélobondo uranium body

A 2D section of approximately 1100×600 m^2 with a WSW-ENE trend and including the Okélobondo ore body (Gabon) was selected for modeling. The conceptual model was divided into six different lithological domains (Fig. 5): FB-pelites, dolomitic complexes, Mn-deposits, the uranium body, FA-sandstones and a basement fault area. The 2D space was discretized into 269 nodes and 489 triangular elements of variable area. The piezometric head was assumed to be equal to the topo-

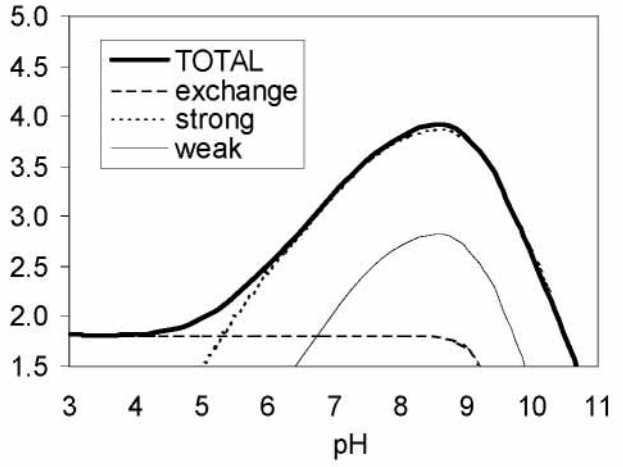

FIGURE 3| **Calculated Ni sorption versus pH in Na montmorillonite for I=0.1. The figure shows the contribution of the different sorption sites.**

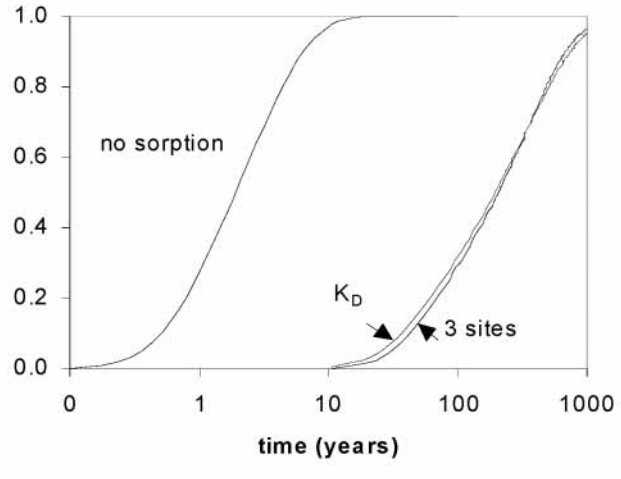

FIGURE 4| **Breakthrough curves for a conservative solute (no sorption) and for Ni according to the 3 sites model described in the text (pH=7; I= 0.1 M; Dif. Coef.= 10^{-8} m²/s). The equivalent K_D retardation curve is included for validation purposes.**

graphy in the upper boundary, whereas no flux was imposed on the rest of the boundaries. As expected from the imposed boundary conditions, the isopotential lines indicate the existence of two convective cells formed by a topography-driven flow. The water recharges in the higher topographic levels and discharges into de Mitembé river.

Thirteen primary species and twenty-six additional aqueous complexes were selected to describe the pore aqueous solution in the Okélobondo system (Table 2). The equilibrium constants for all the aqueous speciation and mineral solubility were those from the EQ3NR data file (Wolery, 1992). The composition of the aquifer lithologies was described with the following minerals: illite, smectite, chlorite, $Fe(OH)_3$(am), kaolinite, plagioclase, K-feldspar, dolomite, rhodochrosite, pyrolusite, manganite, quartz, chalcedony and uraninite.

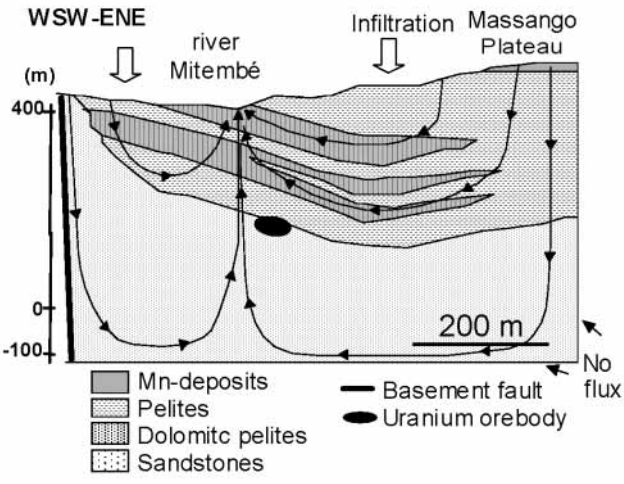

FIGURE 5| **Lithologic domains and groundwater flux sketch of the Okélobondo system.**

After $2 \cdot 10^4$ years the concentration of the solution in all the nodes is constant. For larger times, the only variation is the amount of dissolved or precipitated mineral, i.e., a quasi stationary state is reached. This situation will continue until a mineral disappears. Also, mineral dissolution or precipitation can change porosity, hydraulic conductivity and, consequently, the flow pattern, which in its turn affects reactive transport. However, we assumed that these changes are slow with respect to the time to reach quasi stationary state. For the sake of simplicity, only the mass of the silicates dissolved/precipitated are discussed here. For a complete record of minerals and composition of the solution see Salas (2002).

Chlorite dissolution takes place along the fracture in the WSW boundary and along the pelite lithologies in the surface of the central and E side of the system. The dissolution of chlorite in the fracture of the WSW side and in the superficial pelites causes a slow increase in pH and in the Fe^{2+} concentration. A maximum of chlorite precipitation is predicted in sandstones, close to the WSW fracture. This is linked to the dissolution of illite, as discussed below.

There are two local areas of illite dissolution (Fig. 6). The water infiltrating the WSW part of the system dissolves illite and precipitates chlorite according to the reaction:

$$\text{Illite} + 15.48\ H_2O + 3.08\ Mg^{2+} + 1.67\ Fe^{2+} \rightarrow$$

$$\text{Chlorite} + 0.3\ Al(OH)_4^- + 0.5\ SiO_2(aq) + 0.6\ K^+ + 9.2\ H^+$$

where the excess of Mg^{2+} and the deficit of H^+ results from the upstream dissolution of dolomite. Dissolution of illite and precipitation of kaolinite also take places at the mixing zone of the ENE and WSW cells. The water from the two cells are near-saturation in illite, but the supply of aluminum from the ENE cell, and the more acidic water of the WSW cell induces the reaction:

$$2.5\ \text{Illite} + 1.85\ Al(OH)_4^- + 4.6\ H^+ \rightarrow 3.8\ \text{Kaolinite} + 1.15\ SiO_2(aq) + 0.625\ Mg^{2+} + 1.5\ K^+ + 1.7\ H_2O$$

The water infiltrating the ENE part of the system dissolves plagioclase from the pelites according to the reaction:

$$\text{Plagioclase} + 3.2\ H_2O \rightarrow 1.55\ Al(OH)_4^- + 2.45 SiO_2(aq) + 0.45\ Na^+ + 0.55\ Ca^{2+}$$

The SiO_2(aq) precipitates as amorphous SiO_2, and the excess of aluminum is in part carried away by the water

TABLE 2 | **Aqueous species and kinetic laws used for mineral dissolution (at 25ºC). Equilibrium constants from EQ3NR datafile (version R10, Wolery, 1992). Dissolution/precipitation rates are in mol s^{-1} m^{-2} (moles of mineral per time per reactive surface of the mineral). Activities are in mol kg^{-1}. Data for mineral dissolution kinetics compiled in Salas (2002).**

Primary aqueous species:	
H_2O, Al $(OH)_4^-$, Na^+, Ca^{2+}, Mg^{2+}, Mn^{2+}, K^+, Fe^{2+}, SiO_2(aq),$UO_2(CO_3)_2^{2-}$, HCO_3^-, H^+, e^-	
Aqueous complexes:	
OH^-, Al^{3+}, $Al(OH)_3$(aq), $Al(OH)_2^+$, $AlOH^{2+}$, CO_3^{2-}, CO_2(aq), O_2(aq), $CaCO_3$(aq), Mn^{3+}, $MnCO_3$(aq), MnO_4^{2-}, MnO_4^-, $Mn_2(OH)^{3+}$, Fe^{3+}, $Fe(OH)_{3(aq)}$, $Fe(OH)_2^+$, $FeHCO_3^+$, $Fe(OH)_4^-$, $FeCO_3$(aq), $UO_2(CO_3)^{4-}$, UO_2^{2+}, $U(OH)_4$ (aq), UO_2CO_3 (aq), UO_2OH^+, $UO_2(OH)_2$ (aq)	
Minerals	*Dissolution rate laws at 25°C*
Illite $K_{0.6}Mg_{0.25}Al_{1.8}Al_{0.5}Si_{3.5}O_{10}(OH)_2$	= muscovite
Chlorite $Fe_{1.67}Mg_{3.33}Al_2Si_3O_{10}(OH)_8$	= muscovite
Muscovite	$(4.2\cdot10^{-12}a_H^{0.38} + 1.5\cdot10^{-13}a_H^{0.09} + 1.1\cdot10^{-15}a_H^{-0.22})$ $(\Omega - 1)$
Kaolinite $Al_2Si_2O_5(OH)_4$	$(1.7\cdot10^{-11}a_H^{0.5} + 2.5\cdot10^{-17}a_H^{-0.3})$ $(\Omega - 1)$
Chalcedony SiO_2(am)	precipitation in equilibrium
Pyrolusite MnO_2	precipitation in equilibrium
$Fe(OH)_3$(am)	precipitation in equilibrium
Quartz SiO_2	$4.1\cdot10^{-14}$ $(\Omega - 1)$
Uraninite UO_2	$(1.4\cdot10^{-8}a_H^{0.53} + 10^{-12})$ $(\Omega - 1)$
Rhodochrosite $MnCO_3$	= calcite
Calcite $CaCO_3$	$4.64\cdot10^{-7}$ $(\Omega - 1)$
Manganite MnOOH	10^{-10} $(\Omega - 1)$ (assumed)
Dolomite $CaMg(CO_3)_2$	$2.2\cdot10^{-8}$ $(\Omega - 1)$
Smectite $Ca_{0.20}Na_{0.15}K_{0.2}Fe_{0.85}Mg_{0.55}Al_{1.25}Si_{3.75}O_{10}(OH)_2$	$(10^{-9}a_H^{0.38} + 10^{-13}a_H^{-0.22})$ $(\Omega^{0.1} - 1)^{13}$
K-Feldspar $KAlSi_3O_8$	$(10^{-10}a_H^{0.5} + 2.5\cdot10^{-17}a_H^{-0.45})$ $(\Omega - 1)$
Plagioclase $Ca_{0.55}Na_{0.45}Al_{1.5}Si_{2.5}O_8$	$(7.5\cdot10^{-10}a_H^{0.5} + 1.2\cdot10^{-14}a_H^{-0.30})$ $(\Omega - 1)$

and in part precipitates as illite. As a result, illite precipitation matches the plagioclase dissolution along the schist lithology (Fig. 6). Kaolinite is formed on the surface and along the WSW fault at the expense of the dissolution of the remaining silicates due to the more acidic and diluted superficial waters (Fig. 6).

Observe the illite and kaolinite zones which have a circular shape (Fig. 6). This is a spurious effect due to the high dispersivities that had to be used in order to avoid numerical oscillations. In reality the mixing zone has the shape of a fringe. The problem is that RETRASO uses an Eulerian method for the spatial discretization of the advective and dispersive terms in the transport equation (25). In order to obtain a stable solution, this method must satisfy the Peclet criterion, i.e., the grid spacing should not exceed twice the longitudinal dispersivity in the direction of flow (Daus et al., 1985). The avoidance of numerical oscillations is particularly important for reactive models because negative concentration values would cause the solution to fail. Another constraint is the computational cost, which can be very high in the case of reactive models. As a compromise, in order to avoid numerical oscillations and to keep computation costs within reasonable limits, we selected longitudinal dispersivities in the range of 5-10 m in the reactor area and in the upper lithologies, and 50-70 m at the lower edge of the FA-sandstone. In this lithology, mineral dissolution-precipitation processes were not quantitatively important. Although these values are on the high side, they are still reasonable; the largest being about 1/20 the length of the flow domain, and the smallest being about 1/20 the size of formations represented in the model. The transverse dispersivities are in the range of 1/2-1/5 the longitudinal values. This choice is too large for realistic system, but the used values are on the limit of numerical stability in our model.

Pyrite weathering

This example models the weathering of pyrite (FeS_2) in an unsaturated medium. An important mechanism is the diffusion through the gas phase of atmospheric O_2 that oxidizes the pyrite. The model presented here is a simplified model of that presented by Ayora et al. (2001) and Saaltink et al. (2002). It uses a one-dimensional domain of 0.3 m. The first 0.2 m contains a mixture of sandy soil and pyrite and the remaining 0.1 m only soil. The domain has been discretized into 30 elements of 1 cm.

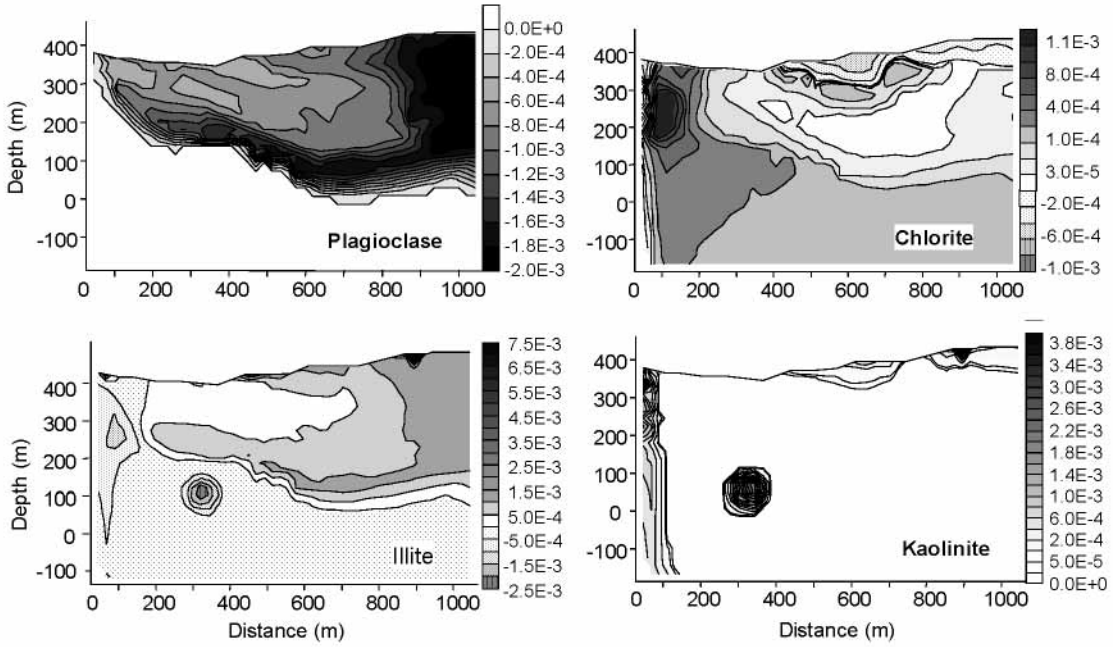

FIGURE 6 | **Mineral dissolution (<0) and precipitation (>0) zones in the Okélobondo uranium boby 2D model (units in mol/m³ rock) after $2 \cdot 10^4$ years. Modified from Salas (2002).**

It has a Darcy flow of 0.1 m year^{-1} constant in time and space. The retention curve and relative permeability were chosen in such a way that a constant saturation was obtained. We used two saturation values, 0.33 and 0.99. The first represents dry and the second wet conditions.

Pyrite can be oxidized through two chemical reactions (Singer and Stumm, 1970; Nicholson, 1994; Nordstrom and Alpers, 1999): Oxidation by oxygen:

$$FeS_2 + 3.5O_2 + H_2O \rightarrow Fe^{2+} + 2SO_4^{2-} + 2H^+ \qquad R1$$

and oxidation by Fe^{3+}:

$$FeS_2 + 14Fe^{3+} + 8H_2O \rightarrow 15Fe^{2+} + 2SO_4^{2-} + 16H^+ \qquad R2$$

Oxidation of Fe^{2+} by O_2 normally has to precede the last reaction:

$$Fe^{2+} + 0.25O_2 + H^+ \rightarrow Fe^{3+} + 0.5H_2O \qquad R3$$

The chemical reactions R1 to R3 are considered to follow a kinetic approach. Kinetic reactions are characterized by the reaction rate (r), which is defined as the amount of reactants evolving to products per unit time. Rate laws express the rate as a function of concentration. We used the following rate laws for reactions R1 to R3:

$$r_1 = 10^{-8.19}\,\sigma\,[O_{2(aq)}]^{0.50}\,[H^+]^{-0.11} \qquad R1$$

$$r_2 = 10^{-6.07}\,\sigma\,[Fe^{3+}]^{0.93}\,[Fe^{2+}]^{-0.40} \qquad R2$$

$$r_3 = 10^{6.02}[Fe^{2+}][O_{2(aq)}][OH^-]^2 + 10^{-8.88}[Fe^{2+}][O_{2(aq)}] \qquad R3$$

where [ ] represents concentrations in mole m^{-3}, σ is the reactive surface of pyrite in m^2 m^{-3}. The rates are given in mole m^{-3} s^{-1}. We used a reactive surface of 10^3 m^2 m^{-3}, calculated from grain size and amount of pyrite in the soil. The rates for reactions R1 and R2 were taken from Nicholson (1994) and that of R3 from Singer and Stumm (1970). The rate for R3 considers only the abiotic reaction. Bacteria may accelerate this reaction by a factor of 10^5-10^6 (Singer and Stumm, 1970; Nordstrom and Alpers, 1999). Therefore, we also calculated a case where the rate is simply 10^6 times higher. Furthermore, we assume the following aqueous reactions to be in equilibrium:

$$OH^- + H^+ \leftrightarrow H_2O$$
$$FeSO_4(aq) \leftrightarrow Fe^{2+} + SO_4^{2-}$$
$$Fe(OH)_3(aq) \leftrightarrow Fe^{3+} + 3OH^-$$
$$NaSO_4^- \leftrightarrow Na^+ + SO_4^{2-}$$
$$H_2S + O_2 \leftrightarrow SO_4^{2-} + 2H^+$$
$$HS^- + O_2 \leftrightarrow SO_4^{2-} + H^+$$

Finally, there are three minerals for which equilibrium is assumed: Na-jarosite ($NaFe_3(SO_4)_2(OH)_6$), ferrihydrite ($Fe(OH)_3$), and melanterite ($FeSO_4 \cdot 7H_2O$).

Figure 7 shows the results of the simulation with only abiotic oxidation of Fe^{II}. It can be clearly seen that a higher saturation value leads to less oxygen diffusion and to lower oxidation rates, higher pH and lower Fe and SO_4 concentrations. Further note, that oxidation of pyrite by O_2 (R1) is several orders of magnitude higher

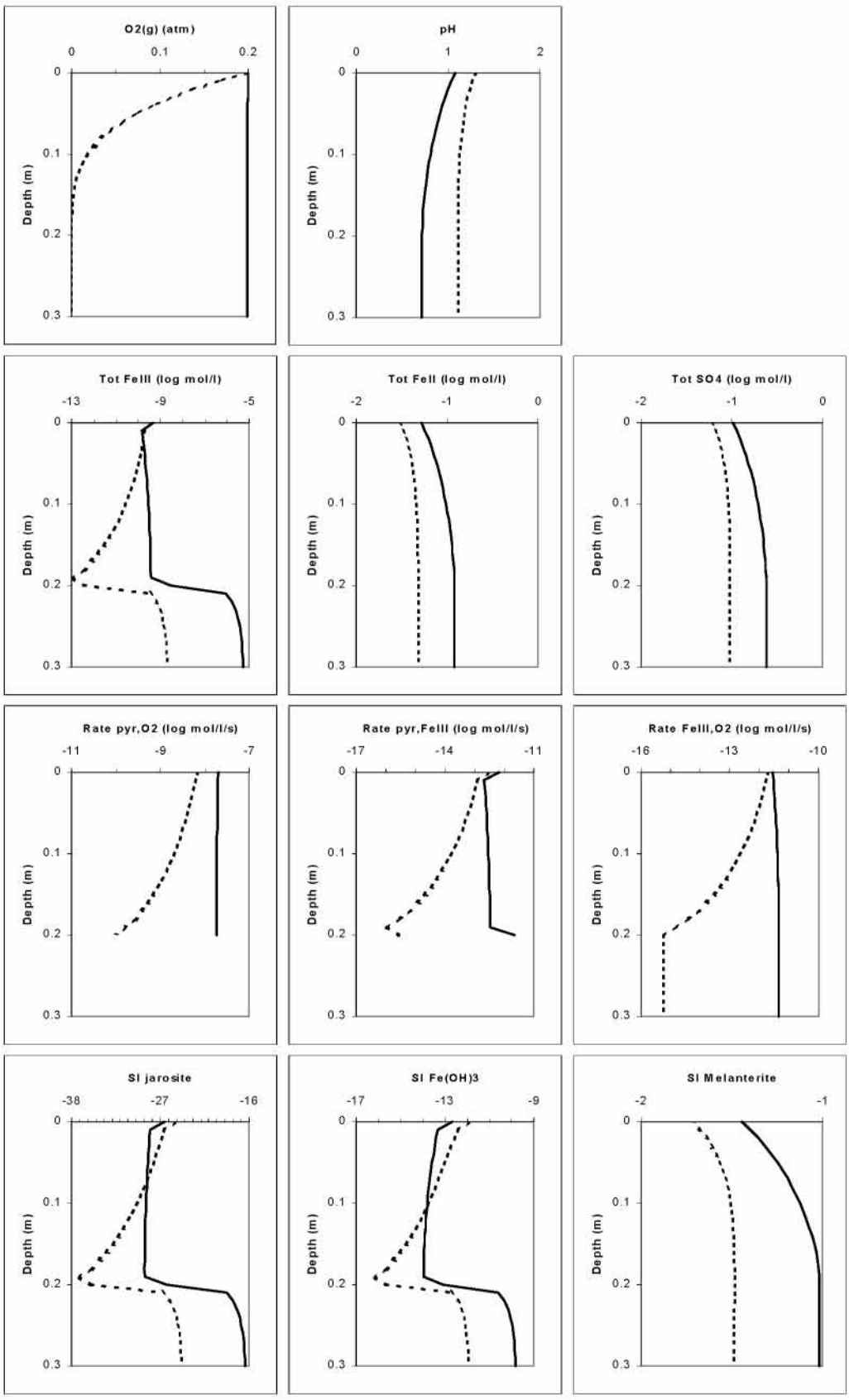

FIGURE 7 | **Results of the pyrite oxidation model with only abiotic oxidation of Fe^{II}. Discontinuous lines refer to saturation of 0.99 and continuous lines to that of 0.33. Note the log scales.**

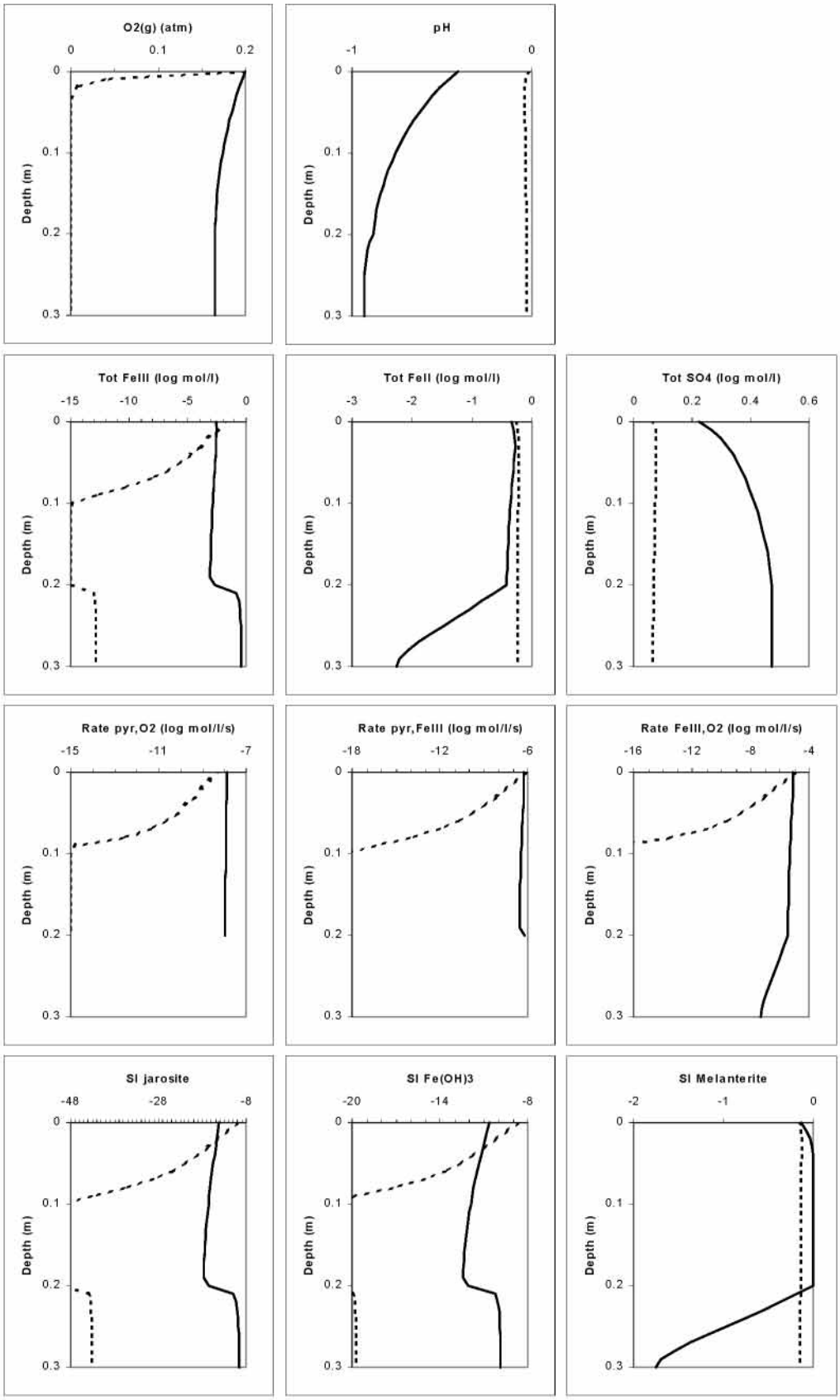

FIGURE 8 | **Results of the steady state model with abiotic and biotic oxidation of Fe^{II}. Discontinuous lines refer to saturation of 0.99 and continuous lines to that of 0.33. Note the log scales.**

than that by Fe^{III} (R2). The reason is not the slowness of the last but the lack of Fe^{III}, which in its turn is caused by the slowness of the oxidation of Fe^{II} by O_2 (R3). Evidence of this is the high concentration of Fe^{II} with respect to Fe^{III} and the fact that Fe^{III} concentrations rise in the lowest 0.1 m where no pyrite is present. Besides, the rate of reaction R3 is always about 14 times higher than that of R2, which coincides with the stoichiometry of both reactions (R2 consumes 14 moles of Fe^{III} in comparison with 1 mole produced by R3). Finally, observe that the saturation indices of all minerals in equilibrium show subsaturation. For Na-jarosite and ferrhydrite this is due to the low pH and the relative low concentrations of Fe^{III}.

Figure 8 displays the results of the simulation that both consider abiotic and biotic oxidation of Fe^{II} (i.e., 10^6 times higher rate constant). For this case the oxidation of pyrite by Fe^{III} (R2) is about one order of magnitude higher than that by O_2 (R1). In comparison to Fig. 7, the higher rate of reactions R2 and R3 causes pH and O_2 concentrations to be lower and Fe and SO_4 concentrations to be higher. The Fe^{III} concentrations are still low in comparison to Fe^{II}, although to a lesser amount as in figure 8. Saturation indices of Na-jarosite and ferrihydrite show subsaturation, but in the presence of pyrite, saturation indices of melanterite equals zero, which means that this mineral is precipitating.

CONCLUSIONS

Complex natural processes can be modeled by coupling interdependent physico-chemical laws for flow of liquid and gas, solute transport processes and chemical reactions. These types of models are essential for the study of processes taking place in soil and groundwater and the impact of human activities on these processes. By changing particular parameters of the model, we can asses the influence of each process on the final outcome. For instance, water saturation has an important effect on the diffusion of O_2 and, as a result, on pyrite oxidation rates (Figs. 7 and 8). Besides, modeling can be used to discuss quantitatively processes occurring at large depths and at geological time scales, for which direct observations are not available.

We have developed a comprehensive tool to model these processes. It can handle both saturated and unsaturated flow, heat transport and reactive transport in both liquid and gas. Possible chemical reactions of the new tool include aqueous complexation, (including redox reactions), adsorption, precipitation-dissolution of minerals and gas dissolution. Precipitation-dissolution and aqueous complexation can be modeled in equilibrium or according to kinetic laws. One, two and three-dimensional finite elements can be used for the spatial discretization.

Nevertheless, the code can still be improved. As shown at the Okélobondo example (Fig. 6), the need to use high dispersivity for numerical reasons may produce spurious results. This need can be avoided by using a Lagrangian formulation for the transport equation instead of the Eulerian formulation, which was used for the presented examples. Batlle et al. (2002) applied successfully a Lagrangian formulation to reactive transport examples. Another improvement of the code can be obtained by adding laws that describe other relations between physical and chemical properties than those described in this paper. Such relationships may include the change of porosity and permeability due to precipitation or dissolution of minerals, the effect of temperature on chemical equilibrium and kinetic constants and the production or consumption of heat due to chemical reactions.

ACKNOWLEDGEMENTS

This work was funded by the project REN2000-1003-C03/HID, by a "Ramón y Cajal" grant of the Spanish Ministry of Science and Technology and by a contract with ENRESA (Spanish Nuclear Waste Company). The comments of Wilfried Pfingsten and Jan van der Lee to improve the quality of the paper are highly appreciated.

REFERENCES

Abu-El-Sha'r, W., Abriola, L.M., 1997. Experimental assessment of gas transport mechanisms in natural porous media: Parameter evaluation. Water Resources Research, 33, 505-516.

Appelo, C.A.J., Willemsen, A., 1987. Geochemical calculations and observations on salt water intrusions, I. A combined geochemical/mixing cell model. Journal of Hydrology, 94, 313-330.

Appelo C.A.J., Postma, D., 1994. Geochemistry, groundwater and pollution. Rotterdam, ed. Balkema, 536 pp.

Ayora, C., Taberner, C., Saaltink, M.W., Carrera, J., 1998. The genesis of dedolomites: a discussion based on reactive transport modeling. Journal of Hydrology, 209, 346-365.

Ayora, C., Berettino, D., Domènech, C., Fernández, M., López-Pamo, E., Olivella, S., de Pablo, J., Saaltink, M.W., 2001. Meteorización de los lodos piríticos de Aznalcóllar. Boletín Geológico y Minero, 112, 137-162.

Baeyens, B., Bradbury, M.H., 1997. A mechanistic description of Ni and Zn sorption on Na-montmorillonite. Part I: Titration and sorption measurements. Journal of Contaminant Hydrology, 27, 223-248.

Baehr, A.L., Baker, R.J., 1995. Use of a reactive gas transport model to determine rates of hydrocarbon biodegradation in unsaturated porous media. Water Resources Research, 31, 2877-2882.

Bain J.G., Blowes D.W., Robertson W.D., Frind E.O., 2000. Modelling of sulfide oxidation with reactive transport at a mine drainage site. Journal of Contaminant Hydrology, 41, 23-47.

Batlle, F., Carrera, J., Ayora, C., 2002. A comparison of Lagrangian and Eulerian formulations for reactive transport modelling. In: Hassanizadeh, S.M., Schotting, R.J., Gray, W.G., Pinder, G.F. (eds.). Computational Methods in Water Resources, Amsterdam, ed. Elsevier, 571-578.

Bradbury, M.H., Baeyens, B., 1997. A mechanistic description of Ni and Zn sorption on Na-montmorillonite. Part II: modelling. Journal of Contaminant Hydrology, 27, 199-222.

Cederberg, G.A., Street, R., Leckie, J.O., 1985. A groundwater mass transport and equilibrium chemistry model for multicomponent systems. Water Resources Research, 21, 1095-1104.

Chilakapati, A., Ginn, T., Szecsody, 1998. An analysis of complex reactions networks in groundwater modeling. Water Resources Research, 34, 1767-1780.

Corbella M., 2002. Modelització geoquímica de dissolució de carbonats per mescles de fluids hidrotermals aplicada a dipòsits minerals. Doctoral thesis, Universitat Autònoma de Barcelona, 130 pp.

Daus, A.D., Frind, E.O., Sudicky, E.A., 1985. Comparative error analysis in finite element formulations of the advection-dispersion equation. Advances in Water Resources, 8, 86-95.

Dzombak, D.A., Morel, F.M.M., 1990. Surface Complexation Modelling. New York, ed. Wiley Interscience, 393 pp.

Engesgaard, P., Kipp, K.L., 1992. A Geochemical Transport Model for Redoxed-Controlled Movement of Mineral Fronts in Groundwater Flow Systems: A Case of Nitrate Removal by Oxidation of Pyrite. Water Resources Research, 28, 2829-2843.

Engesgaard, P., Traberg, R., 1996. Contaminant transport at a waste residue deposit, 2. Geochemical transport modeling. Water Resources Research, 32, 939-951.

Friedly, J.C., Rubin, J., 1992. Solute transport with multiple equilibrium controlled or kinetically controlled chemical reactions. Water Resources Research, 28, 1935-1953.

Gerke H.H., Molson J.W., Frind E.O., 1998. Modelling the effect of chemical heterogeneity on acidification and solute leaching in overburden mine spills. Journal of Hydrology, 209, 166-185.

Grindrod, P., Takase, H., 1996. Reactive chemical transport within engineered barriers. Journal of Contaminant Hydrology, 21, 283-296.

Helgeson, H.C., Kirkham, D.H., 1974. Theoretical prediction of the thermodynamic behaviour of aqueous electrolytes at high pressures and temperatures: II. Debye-Hückel parameters for activity coefficients and relative partial molal properties. American Journal of Science, 274, 1199-1261.

Le Gallo, Y., Bildstein O., Brosse, E., 1998. Coupled reaction-flow modeling of diagenetic changes in resevoir permeability, porosity and mineral composition. Journal of Hydrology, 209, 366-388.

Liu, C.W., Narasimhan, T.N., 1989a. Redox-Controlled multiple-species reactive chemical transport, 1. Model Development. Water Resources Research, 25, 869-882.

Liu, C.W., Narasimhan, T.N., 1989b. Redox-controlled multiple species reactive chemical transport, 2. Verification and Application. Water Resources Research, 25, 883-910.

Mangold, C.M., Tsang, C.H., 1991. A summary of subsurface hydrological and hydrochemical models. Reviews in Geophysics, 29, 51-79.

Mayer, K.U., Frind, E.O., Blowes, D.W., 2002. Multicomponent reactive transport modeling in variably saturated media using a generalized formulation for kinetically controlled reactions. Water Resources Research, 38, doi:10.1029-/2001WR000862.

Nicholson, R.V., 1994. Iron-sulfide oxidation mechanisms: Laboratory studies. In: Jambor, J.L., Blowes, D.W., (eds.). Short course on environmental geochemistry of sulfide mine-wastes, , Waterloo, Ottawa, Mineralogical Association of Canada, 163-183.

Nienhuis, P., Appelo, C.A.T., Willemsen, A., 1991. Program PHREEQM: Modified from PHREEQM for use in mixing cell flow tube.

Nordstrom, D.K., Alpers, C.N., 1999. Geochemistry of acid mine water. In:. Plumlee, G.S., Logsdon, M.J. (eds.). The environmental geochemistry of mineral deposits, Part A: Processes, techniques and health issues. Littleton, Colorado, Society of Economic Geologists, chapter 6.

Olivella, S., Gens, A., Carrera, J., Alonso, E.E., 1996. Numerical formulation for a simulator (CODE_BRIGHT) for the coupled analysis of saline media. Engineering Computations, 13, 87-112.

Parkhurst, D.L., 1995. User's guide to PHREEQC: a computer program for speciation, reaction-path, advective-transport and inverse geochemical calculations. U.S. Geolocial Survey, Water Resources Investigation Report, 95-4227, 143 pp.

Rovira M., El Aamrani, F.Z., Duro, L., Casas, I., de Pablo, J., Bruno, J., Domènech, C., Ayora, C., 2000. Experimental study and modeling of uranium (VI) transport through ferrous olivine rock columns. Radiochimica Acta, 88, 1-7.

Rubin, J., 1983. Transport of reacting solutes in porous media: Relation between mathematical nature of problem formulation and chemical nature of reactions. Water Resources Research, 19, 1231-1252.

Saaltink, M., Benet, I., Ayora, C., 1997. RETRASO, Fortran Code for Solving 2D Reactive Transport of Solutes, Users´s guide. Barcelona, E.T.S.I. Caminos, Canales y Puertos, Universitat Politècnica de Catalunya and Instituto de Ciencias de la Tierra, CSIC, 90 pp.

Saaltink, M.W., Ayora,C., Carrera, J., 1998. A mathematical formulation for reactive transport that eliminates mineral concentration. Water Resources Research, 34, 1649-1656.

Saaltink, M.W., Carrera, J., Ayora,C., 2001. On the behavior of approaches to simulate reactive transport. Journal of Contaminant Hydrology, 48, 213-235.

Saaltink, M.W., Domènech, C., Ayora, C., Carrera, C., 2002. Modelling the oxidation of sulphides in an unsaturated soil. In:. Younger, P., Robins, N.S. (eds.). Mine Water Hydrogeology and Geochemistry, London, Geological Society, Special Publications, 198, 187-205.

Saaltink, M.W., Ayora, C., Stuyfzand, P.J., Timmer, H., 2003. Analysis of a deep well recharge experiment by calibrating a

reactive transport model with field data. Journal of Contaminant Hydrology, 65, 1-18.

Salas J., 2002. Modelación del transporte reactivo en los yacimientos de uranio de la cuenca Franceville. Doctoral thesis, Universidat de Barcelona, 195 pp.

Schäfer, D., Schäfer, W., Kinzelbach, W., 1998. Simulation of reactive processes related to biodegradation in aquifers, 1. Structure of the three-dimensional reactive transport model. Journal of Contaminant Hydrology, 31, 167-186.

Šimůnek, J., Suarez, D.L., 1994. Two-dimensional transport model for variability saturated porous media with major ion chemistry. Water Resources Research, 30, 1115-1133.

Singer, P.C., Stumm, W., 1970. Acidic mine drainage: The determining step. Science, 167, 1121-1123.

Steefel, C.I., 1993. 1DREACT, One dimensional reaction-transport model, User manual and programmer's guide. Batelle, Washington, Pacific Northwest Laboratories.

Steefel, C.L., Lasaga, A.C., 1994. A coupled model for transport of multiple chemical species and kinetic precipitation/dissolution reactions with application to reactive flow in single phase hydrothermal systems. American Journal of Science, 294, 529-592.

Steefel, C.I., Yabusaki, S.B., 1995. OS3D/GIMRT, Software for modeling multicomponent-multidimensional reactive transport, User manual & programmer´s guide. Richland, Washington, Pacific Northwest Laboratories, 58 pp.

Steefel, C.I., MacQuarrie, K.T.B., 1996. Approaches to modeling reactive transport in porous media. In: Lichtner, P.C., Steefel, C.I., Oelkers, E.H. (eds.). Reactive transport in porous media. Mineralogical Society of America, Reviews in Mineralogy, 34, 83-129.

Tebes-Stevens, C., Valocchi, A.J., VanBriesen, J.M., Rittmann, B.E., 1998. Multicomponent transport with coupled geochemical and microbiological reactions: model description and example simulation. Journal of Hydrology, 209, 8-26.

Thorstenson, D.C., Pollock, D.W., 1989. Gas transport in unsaturated zones: multicomponent systems and the adequacy of Fick's laws. Water Resources Research, 25, 477-507.

Van der Lee, J., De Windt, L., 2001. Present state and future directions of modeling of geochemistry in hydrogeological systems. Journal of Contaminant Hydrology, 47, 265-282.

Van der Lee, J., De Windt, L., Lagneau, V., Goblet P., 2003. Module-oriented modeling of reactive transport with HYTEC. Computer and Geosciences, 29, 265-275.

Van Genuchten, R., 1978. Calculating the unsaturated hydraulic conductivity with a new closed-form analytical model. Research report 78-WR-08, Water Resource Program, Princeton, NJ, Department of Civil Engineering, Princeton University, 63 pp.

Van Genuchten, M.T.H., Alves, W.J., 1982. Analytical solutions of the one-dimensional convective-dispersive solute transport equation. U.S. Department of Agriculture, Technical Bulletin, 1661, 151 pp.

Walter, A.L., Frind, E.O., Blowes, D.W., Ptacek, C.J., Molson, J.W., 1994. Modeling of multicomponent reactive transport in groundwater, 1. Model development and evaluation. Water Resources Research, 30, 3137-3148.

Westall J.C., Hohl H., 1980. A comparison of electrostatic models for the oxide/solution interface. Advances in Colloid and Interface Science, 12, 265-294.

White, S.P., 1995. Multiphase nonisothermal transport of systems of reacting chemicals. Water Resources Research, 31, 1761-1772.

Wolery T.J., 1992. EQ3NR, a computer program for geochemical aqueous speciation-solubility calculations: Theoretical manual, user's guide and related documentation (Version 7.0). Publ. UCRL-MA-110662 Pt III. Livermore, California, Lawrence Livermore Lab., 246 pp.

Wunderly, M.D., Blowes, D.W., Frind, E.O., Ptacek, C.J., 1996. Sulfide mineral oxidation and subsequent reactive transport of oxidation products in mine tailing impoundments: a numerical model. Water Resources Research, 32 , 3173-3187.

Xu, T., Samper, J., Ayora, C., Manzano, M., Custodio, E., 1999. Modeling of non-isothermal multi-component reactive transport in field scale porous media flow systems. Journal of Hydrology, 214, 144-164.

Yeh, G.T., Tripathi, V.S., 1989. A critical evaluation of recent developments in hydrogeochemical transport models of reactive multichemical components. Water Resources Research, 25, 93-108.

Yeh, G.T., and Tripathi, V.S., 1991. A model for simulating transport of reactive multispecies components: model development and demonstration. Water Resources Research, 27, 3075-3094.

Manuscript received March 2003;
revision accepted December 2003.